

## High-Order Harmonic Generation in Xenon at 1064 nm: The Role of Phase Matching

A. L'Huillier,<sup>(1)</sup> K. J. Schafer,<sup>(2)</sup> and K. C. Kulander<sup>(2)</sup>

<sup>(1)</sup>*Service de Physique des Atomes et des Surfaces, Centre d'Etudes Nucléaires de Saclay, 91191 Gif-sur-Yvette, France*

<sup>(2)</sup>*Lawrence Livermore National Laboratory, University of California, Livermore, California 94550*

(Received 26 July 1990)

We present a completely *ab initio* calculation of harmonic generation in xenon exposed to a strong laser field. The time-dependent Schrödinger equation for the atomic response and the propagation equation are numerically integrated yielding excellent agreement with experiment. The weaker variation with pump intensity of the induced dipole in the high-field regime leads to an enormous enhancement in phase matching compared to the perturbative limit and a defocusing of the generated harmonics.

PACS numbers: 42.65.Ky, 32.80.Rm

Recently, considerable theoretical work has been done on high-order harmonic generation by a single atom exposed to a strong radiation field.<sup>1-6</sup> This has been stimulated by experimental results obtained in the rare gases by Rhodes and co-workers<sup>7</sup> using a KrF laser (248 nm) and by the Saclay group<sup>8</sup> with a Nd-doped yttrium-aluminum-garnet laser (1064 nm). These latter experiments show the production of very-high-order odd harmonics, e.g., up to the 33rd harmonic in Ar at 1064 nm and  $3 \times 10^{13}$  W cm<sup>-2</sup>, with a characteristic intensity distribution: a rapid decrease between the third and the fifth harmonic, a plateau of approximately constant intensities extending from the fifth or seventh harmonic to a high-order harmonic, and finally a cutoff. Most calculations of the emission spectrum of individual atoms in strong fields which go beyond perturbation theory qualitatively reproduce this behavior.<sup>1-6</sup> This result is surprising since the observation of harmonic generation requires that in addition to strong single-atom emission there be proper phase matching between the induced and driving fields. Phase matching can depend strongly on the order of the nonlinear process, leading to the expectation that the single-atom and macroscopic spectra will have very different distributions. In fact, quite general considerations lead to the conclusion that any plateau in the single-atom response should be destroyed by the effect of propagation in a focused-beam geometry.<sup>9</sup> Here we do three things: We present the first *ab initio* calculation of high-order harmonic generation in a rare gas taking account of both the single-atom response and propagation effects in a nonperturbative way, and compare the results to experimental data;<sup>10</sup> we explain the role of phase matching in a strong-field regime and resolve the paradox presented above; and we discuss the implication of our results for future experiments.

Phase matching is traditionally addressed in terms of the variation of the *phases* of the interfering fields throughout the nonlinear medium.<sup>11-13</sup> Two effects are important: dispersion, since waves at different frequencies travel at different speeds in the medium and therefore get out of phase with each other, and focusing. Focusing introduces a geometrical phase slip, which is

different for the harmonic field and its driving polarization. The induced phase mismatch increases dramatically with increasing harmonic order. In recent experiments,<sup>8,10</sup> the density was low so the dispersion was small,<sup>9</sup> but the beam was focused to achieve a high intensity. Therefore one would expect, based on the arguments just given, that no plateau (or even any significant number of high harmonics) would be observed. Although these arguments are usually associated with the weak-field limit,<sup>12</sup> they are quite general and it is hard to see how going to a strong-field regime would modify them significantly. The main conclusion of this Letter is that phase matching also depends, in a crucial manner, on how the *amplitudes* of the fields vary throughout the medium. It is in this regard that the strong-field regime differs most strikingly from the weak-field limit. In the latter case, the nonlinear polarization which is proportional to the single-atom response, varies as the  $q$ th power of the incident field,  $q$  denoting the harmonic order. This means that high-order harmonic production is strongly concentrated in the center of the focal volume. In a strong field, the nonlinear polarization varies much less rapidly with the incident field and behaves similarly for all of the harmonics in the plateau. This increases the volume in which the harmonics are generated, balances the rapid loss of coherence brought about by focusing, and leads to constant phase-matching factors for the high harmonics.

To calculate the harmonic yield in the strong-field regime, we solve the propagation equation in the far field using an integral formulation of Maxwell's equations. The  $q$ th harmonic field  $\mathcal{E}_q$  with wave vector  $k_q$  is<sup>14</sup>

$$\mathcal{E}_q(\mathbf{r}') = \left[ \frac{q\omega}{c} \right]^2 \int \frac{e^{ik_q R}}{R} \mathcal{P}_q(\mathbf{r}) d^3r, \quad (1)$$

where  $R = |\mathbf{r} - \mathbf{r}'|$ ,  $\omega$  is the laser frequency, and  $\mathcal{P}_q$  is the nonlinear polarization field. We introduce the slowly varying envelopes  $E_q(\mathbf{r}) = \mathcal{E}_q(\mathbf{r}) \exp(-ik_q z)$  and  $\mathcal{P}_q(\mathbf{r}) = \mathcal{P}_q(\mathbf{r}) \exp(-ik_q z)$ , where  $z$  is the propagation axis, and make the paraxial approximation. The harmonic profile in the far field ( $|z - z'| \gg |x - x'|, |y - y'|$ ) be-

comes an integral over the nonlinear medium:<sup>9,15</sup>

$$E_q(\mathbf{r}') = \left( \frac{q\omega}{c} \right)^2 \int \frac{P_q(\mathbf{r}) \exp(i \int_z^{+\infty} \Delta k dz'')}{z' - z} \exp \left( \frac{ik_q(|x - x'|^2 + |y - y'|^2)}{2(z' - z)} \right) d^3r. \quad (2)$$

Here  $\Delta k = k_q - qk_1$  denotes the ( $z$ -dependent) linear phase mismatch, including absorption.<sup>9</sup> We assume that the  $q$ th harmonic field is produced by the fundamental field and not by other (lower-order) harmonic fields. We can write the incident field as

$$\text{Re}[E_1(r, z) e^{i(k_1 z - \omega t)}] = \text{Re}[|E_1(r, z)| e^{i[k_1 z - \omega t - \varphi(r, z)]}].$$

The polarization field  $P_q$  is then equal to  $2\mathcal{N}(z)d_q(r, z)e^{-iq\varphi(r, z)}$ , where  $\mathcal{N}(z)$  denotes the (local) atomic density and  $d_q(r, z)$  is the  $q$ th harmonic component of the time-dependent dipole moment evaluated for a field strength  $|E_1(r, z)|$ . Note that the geometrical phase  $q\varphi(r, z)$  introduced by focusing depends only on the process order  $q$  and not on the laser intensity.

The single-atom response  $d_q$  is obtained from the wave function generated by numerically integrating the time-dependent Schrödinger equation for an electron in a pseudopotential that describes well the xenon valence orbital.<sup>2,16</sup> It is calculated over a fine intensity grid, between  $0.5 \times 10^{13}$  and  $5 \times 10^{13}$  W cm<sup>-2</sup>. The harmonic components first increase rapidly with the laser intensity (as in the weak-field picture), and then more slowly, with numerous structures and resonances. On average the increase with intensity is much less than expected from lowest-order perturbation theory, particularly at the highest intensities. The single-atom emission spectrum exhibits the plateau structure referred to above.

The macroscopic parameters of the interaction (pressure, focusing, etc.) are chosen to mimic the experimental conditions of Ref. 10. The gas density is described by a Lorentzian in the  $z$  direction with a width at half maximum of  $L = 1$  mm and a maximum density  $\mathcal{N}_0$  equal to  $5.3 \times 10^{17}$  atoms/cm<sup>3</sup> (15 Torr). It is taken to be zero outside a 2-mm interaction length. The incident laser beam is assumed to be Gaussian and we consider two cases with confocal parameters  $b = 4$  or 1 mm. We use a 36-ps Gaussian pulse. For consistency, depletion of the neutral medium due to ionization, which becomes significant above  $2 \times 10^{13}$  W cm<sup>-2</sup>, has been introduced by using ionization rates obtained from the same time-dependent calculations that were used to produce  $d_q$ .

The number of photons emitted at a given harmonic frequency is obtained by integrating the harmonic intensity profile,

$$N_q = \frac{c}{4q\hbar\omega} \int |E_q(r', t)|^2 r' dr' dt.$$

In Figs. 1(a) and 1(b), we compare *in absolute value* calculated and measured yields for several peak laser intensities. The theoretical curves are slightly high, particularly for the highest-intensity result, but are still gen-

erally within the experimental error bars, estimated to be about 1 order of magnitude. The general shape of the harmonic spectrum as a function of the peak laser intensity is very well reproduced by our calculation.

To separate the role of propagation from the single-atom response, we define a phase-matching factor  $\mathcal{F}_q$  by analogy with the weak-field limit as

$$\mathcal{F}_q = 4\hbar N_q / \pi^2 b^3 \tau_q \mathcal{N}_0^2 |d_q|^2, \quad (3)$$

where  $\tau_q$  is the integral of the  $q$ th power of the laser

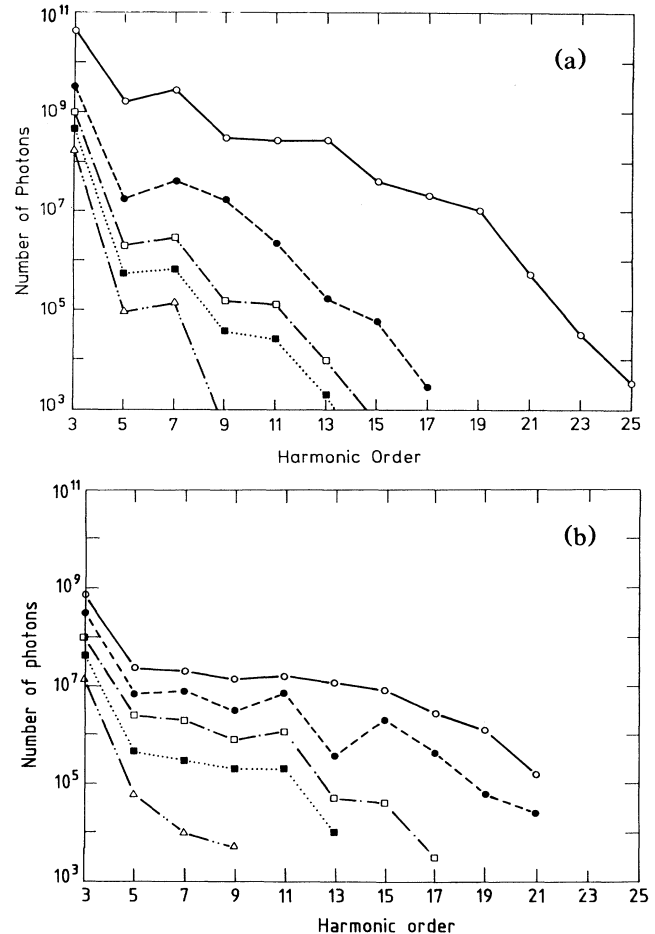


FIG. 1. (a) Calculated number of photons for  $b = 4$  mm,  $L = 1$  mm. (b) Experimental number of photons for the same conditions (Ref. 10). The intensities are from the top to the bottom  $3 \times 10^{13}$  (solid line),  $1.3 \times 10^{13}$  (dashed line),  $0.9 \times 10^{13}$  (dot-dashed line),  $0.7 \times 10^{13}$  (dotted line), and  $0.5 \times 10^{13}$  (double-dot-dashed line) W cm<sup>-2</sup>.

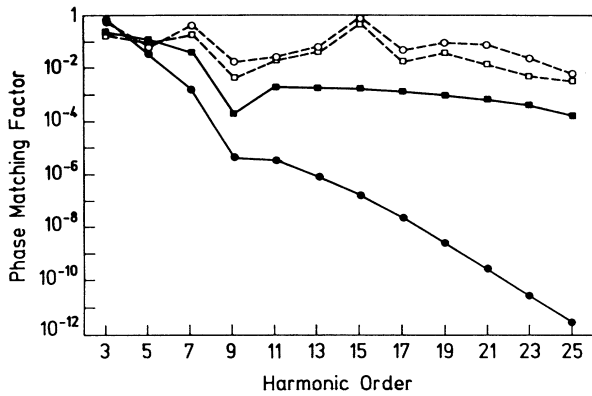


FIG. 2. Phase-matching factor  $\mathcal{F}_q$  as a function of the harmonic order  $q$ . The perturbative results are shown as solid lines, and the strong-field results obtained at  $3 \times 10^{13} \text{ W cm}^{-2}$  as dashed lines. Two geometries have been investigated  $b=1$  mm (circles)  $b=4$  mm (squares).

temporal distribution,  $d_q$  is evaluated at the maximum laser intensity, and ionization is excluded. Figure 2 compares  $\mathcal{F}_q$  for two focusing geometries and two laser intensities. In the weak-field limit,  $\mathcal{F}_q$  can be calculated from perturbation theory. It decreases rapidly with increasing order, and is strongly dependent on the geometry (compare the  $b=1$  mm and  $b=4$  mm curves). For example, when  $b$  is equal to the medium interaction length ( $b=L=1$  mm),  $\mathcal{F}_q$  decreases by 12 orders of magnitude from the 3rd to the 25th harmonic. In contrast, in the strong field case at  $3 \times 10^{13} \text{ W cm}^{-2}$ ,  $\mathcal{F}_q$  remains relatively constant, varying between 1 and  $10^{-2}$  over the same range. Moreover, it is relatively insensitive to the focusing geometry, which agrees with the experimental observations.<sup>10</sup>

The large difference between  $\mathcal{F}_q$  in the weak- and strong-field regimes is due to the scaling with intensity of  $d_q$ . To illustrate this, we studied  $\mathcal{F}_q$  as a function of the phase mismatch  $\Delta k$ , both in the weak-field limit, where  $d_q$  is proportional to  $|E_1|^q$ , and in a model situation, where  $d_q$  is assumed to vary as  $|E_1|^5$ . This is approximately the power law found<sup>2</sup> for the single-atom response above  $10^{13} \text{ W cm}^{-2}$ . Figure 3 shows a comparison between perturbative and “strong-field” phase-matching factors for the 5th, 13th, and 21st harmonics, calculated for a tight focusing geometry ( $b=1$  mm). In the weak-field limit and for a square gas jet the phase-matching integral  $F_q$  (with  $\mathcal{F}_q = |F_q|^2$ ) is<sup>12,13</sup>

$$F_q(\Delta k, b) = \int_{-L/2}^{L/2} e^{-i[\Delta k z + (q-1)\tan^{-1}(2z/b)]} \times (1 + 4z^2/b^2)^{(1-q)/2} 2 dz/b. \quad (4)$$

Compared with a plane wave, focusing introduces a phase factor  $(q-1)\tan^{-1}(2z/b)$  and an amplitude term  $(1 + 4z^2/b^2)^{(1-q)/2}$ , which damps the integrand away from the focus. The strong-field model yields an expres-

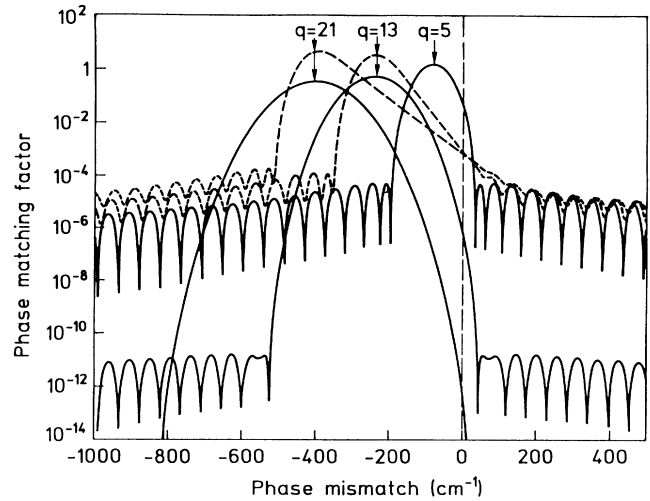


FIG. 3. Phase-matching factor  $\mathcal{F}_q$  for the 5th, 13th, and 21st harmonics as a function of the phase mismatch  $\Delta k$  ( $\text{cm}^{-1}$ ) for  $b=1$  mm and  $L=1$  mm. The solid lines indicate the perturbative results; the dashed lines, results obtained by assuming a fifth-power dependence for the 13th and 21st harmonics.

sion for  $F_q$  that is much more complicated. The phase factor, which is purely geometrical, is roughly the same, particularly in its dependence on  $q$ , the process order. The damping term, however, depends on the effective order of nonlinearity of  $d_q$ , and becomes approximately  $(1 + 4z^2/b^2)^{(1-p)/2}$ , where  $p=5$ .

In both the strong- and weak-field limits, the effective phase mismatch induced by focusing shifts the maximum of  $\mathcal{F}_q$  towards negative  $\Delta k$ . Optimum phase matching can be achieved only for very negatively dispersive media [ $\Delta k \approx 2(1-q)/b$ ]. This condition cannot be satisfied for all harmonics simultaneously because of the dependence on  $q$ . The amplitude factor, which is quite different for the two cases, affects the behavior of the phase-matching function away from its maximum. In the weak-field limit, the rapid damping makes the medium appear, for the high harmonics, essentially as if it were infinite. Recall that for an infinite medium and small coherence length (large effective phase mismatch), the harmonic fields generated before the focus are exactly canceled by those created after the focus, yielding no net harmonic generation. For a finite medium, exact cancellation occurs only for some periodic values of  $\Delta k$ . This leads to the  $(\sin x/x)^2$  type of oscillations in Fig. 3. The average level of those oscillations depends on how rapidly the integrand in Eq. (4) is damped as it reaches the medium boundaries. This is determined by the effective order of nonlinearity of  $d_q$  and not by the process order. Consequently, at the experimental conditions ( $\Delta k \approx 0$ ),  $\mathcal{F}_q$  remains approximately constant. In Fig. 3 the line  $\Delta k=0$  intersects  $\mathcal{F}_q$  at about the same level for the mod-

el 5th, 13th, and 21st harmonics. This will be true as long as the different harmonic components of the dipole moment have approximately the same (low) intensity dependence. Therefore, the efficient phase matching obtained in the strong-field regime is a direct consequence of the weaker damping of the phase-matching integral which follows from the weaker intensity dependence of the single-atom emission at the harmonic frequencies. This is purely an amplitude rather than a phase effect.

Future experiments should be able to offer further evidence of the qualitative difference between the strong- and weak-field regimes. The larger volume within which the higher harmonics are produced leads to a loss of spatial coherence. Therefore, the far-field harmonic intensity profile (which has so far not been measured) becomes narrower as the pump intensity increases. It is approximately Gaussian in a loosely focused geometry ( $b \gg L$ ), but can exhibit rings in a tightly focused geometry ( $b \leq L$ ). From Fig. 3 we also see that even under conditions that result in large positive or negative phase mismatches, such as higher pressure or the presence of many free electrons, the harmonic conversion efficiency will still be high, again in contrast to one's expectation based upon the weak-field limit.

In summary, extending harmonic generation into the strong-field regime has two unexpected and fortunate consequences: A plateau forms in the single-atom response, meaning that generation of, say, the 17th harmonic becomes as probable as the generation of the 5th harmonic; and all the generated harmonics become equally and efficiently phase matched.

We are grateful to P. H. Bucksbaum, R. R. Freeman, S. E. Harris, J. L. Krause, R. M. Potvliege, and B. W. Shore for helpful discussions. This work was performed in part under the auspices of the Department of Energy at the Lawrence Livermore National Laboratory under

Contract No. W-7405-Eng-48.

<sup>1</sup>See references in J. Opt. Soc. Am. B 7 (1990), edited by K. C. Kulander and A. L'Huillier, pp. 502-536.

<sup>2</sup>K. C. Kulander and B. W. Shore, Phys. Rev. Lett. 62, 524 (1989); J. Opt. Soc. Am. B 7, 502 (1990); B. W. Shore and K. C. Kulander, J. Mod. Opt. 36, 857 (1989).

<sup>3</sup>R. M. Potvliege and R. Shakeshaft, Phys. Rev. A 40, 3061 (1989).

<sup>4</sup>G. Bandarage, A. Maquet, and J. Cooper, Phys. Rev. A 41, 1744 (1990).

<sup>5</sup>J. H. Eberly, Q. Su, and J. Javanainen, Phys. Rev. Lett. 62, 881 (1989); J. Opt. Soc. Am. B 6, 1289 (1989).

<sup>6</sup>W. Becker, S. Long, and J. K. McIver, Phys. Rev. A 41, 4112 (1990); B. Sundaram and P. W. Milonni, Phys. Rev. A 41, 6571 (1990).

<sup>7</sup>A. McPherson, G. Gibson, H. Jara, U. Johann, T. S. Luk, I. McIntyre, K. Boyer, and C. K. Rhodes J. Opt. Soc. Am. B 4, 595 (1987).

<sup>8</sup>M. Ferray, A. L'Huillier, X. F. Li, L. A. Lompré, G. Mainfray, and C. Manus, J. Phys. B 21, L31 (1988); X. F. Li, A. L'Huillier, M. Ferray, L. A. Lompré, and G. Mainfray, Phys. Rev. A 39, 5751 (1989).

<sup>9</sup>A. L'Huillier, X. F. Li, and L. A. Lompré, J. Opt. Soc. Am. B 7, 527 (1990).

<sup>10</sup>L. A. Lompré, A. L'Huillier, M. Ferray, P. Monot, G. Mainfray, and C. Manus, J. Opt. Soc. Am. B 7, 754 (1990).

<sup>11</sup>J. F. Ward and G. H. C. New, Phys. Rev. 185, 57 (1969); R. B. Miles and S. E. Harris, IEEE J. Quantum Electron. 9, 470 (1973).

<sup>12</sup>G. C. Bjorklund, IEEE J. Quantum Electron. 11, 287 (1975).

<sup>13</sup>J. F. Reintjes, *Nonlinear Optical Parametric Processes in Liquids and Gases* (Academic, New York, 1984).

<sup>14</sup>J. D. Jackson, *Classical Electrodynamics* (Wiley, New York, 1975), 2nd ed.

<sup>15</sup>A. Lago, G. Hilber, and R. Wallenstein, Phys. Rev. A 36, 3827 (1987).

<sup>16</sup>K. C. Kulander Phys. Rev. A 38, 778 (1988).